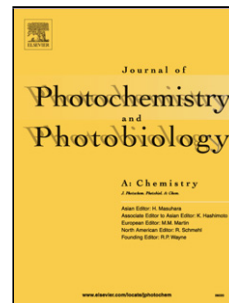


Accepted Manuscript

Title: Long-wavelength absorbing fluorescent polymethine dyes derived from the 6-(*N,N*-diethylamino)-1,2,3,4-tetrahydroxanthylum system

Authors: D.S. Conceição, D.P. Ferreira, Y. Prostota, O.D. Kachkovsky, L.F.Vieira Ferreira, P.F. Santos



PII: S1010-6030(17)30499-9
DOI: <http://dx.doi.org/doi:10.1016/j.jphotochem.2017.07.045>
Reference: JPC 10771

To appear in: *Journal of Photochemistry and Photobiology A: Chemistry*

Received date: 12-4-2017
Revised date: 28-7-2017
Accepted date: 31-7-2017

Please cite this article as: D.S.Conceição, D.P.Ferreira, Y.Prostota, O.D.Kachkovsky, L.F.Vieira Ferreira, P.F.Santos, Long-wavelength absorbing fluorescent polymethine dyes derived from the 6-(*N,N*-diethylamino)-1,2,3,4-tetrahydroxanthylum system, *Journal of Photochemistry and Photobiology A: Chemistry*<http://dx.doi.org/10.1016/j.jphotochem.2017.07.045>

This is a PDF file of an unedited manuscript that has been accepted for publication. As a service to our customers we are providing this early version of the manuscript. The manuscript will undergo copyediting, typesetting, and review of the resulting proof before it is published in its final form. Please note that during the production process errors may be discovered which could affect the content, and all legal disclaimers that apply to the journal pertain.

Long-wavelength absorbing fluorescent polymethine dyes derived from the 6-(*N,N*-diethylamino)-1,2,3,4-tetrahydroxanthylum system

D.S. Conceição^a, D.P. Ferreira^a, Y. Prostota^b, O. D. Kachkovsky^c, L.F.Vieira Ferreira^a,

P.F. Santos^{b,*}

^a*Centro de Química-Física Molecular and IN-Institute of Nanoscience and Nanotechnology, Instituto Superior Técnico, Universidade de Lisboa, Av. Rovisco Pais, 1049-001 Lisboa*

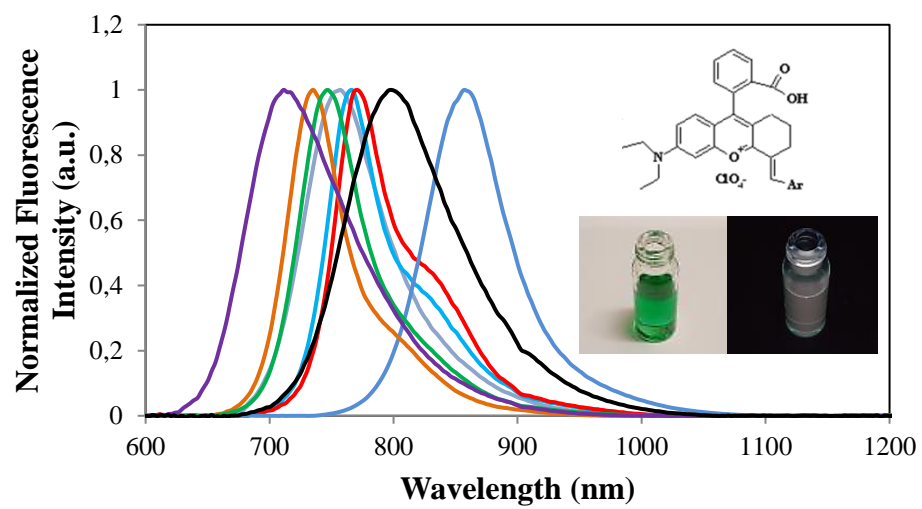
^b*Centro de Química - Vila Real, Universidade de Trás-os-Montes e Alto Douro, 5001-801 Vila Real, Portugal*

^c*Institute of Bioorganic Chemistry and Petrochemistry, National Academy of Sciences of Ukraine, 1 Murmanska str, 02660, Kyiv, Ukraine*

* To whom correspondence should be addressed.

Email: psantos@utad.pt

Keywords: Rhodamines; 1,2,3,4-tetrahydroxanthylum; NIR-dyes; fluorescence quantum yields; fluorescence lifetimes; singlet oxygen.



Abstract

Several new dyes derivatives of the “rhodamine-like” 6-(*N,N*-diethylamino)-1,2,3,4-tetrahydroxanthylum heterocyclic system displaying absorption within the near-infrared were synthesized. The photochemical behaviour of these molecules was evaluated in dichloromethane, regarding their ground state absorption properties, fluorescence emission quantum yields and fluorescence lifetimes determinations. The singlet oxygen quantum yields of the new dyes were also obtained. The absorption and luminescence spectral data showed that the behaviour of these dyes is strongly dependant on the nature of the (hetero)aromatic substituent introduced in the 1,2,3,4-tetrahydroxanthylum scaffold. The performed quantum-chemical calculations indicated that those (hetero)aromatic terminal substituents are practically planar and hence are conjugated with the chromophoric system of the 1,2,3,4-tetrahydroxanthylum framework. Such elongation of total π -system is accompanied by regular delocalization of the frontier MOs and decreasing of the first electron transition energy manifested itself by bathochromic effect in dyes absorption.

1. Introduction

In the last few years, fluorescence-based imaging techniques emerged as one of the most widely tools used for biomolecules monitoring in living systems. Fluorescent probes, more specifically organic dye molecules, possess several properties which make them suitable for single-molecule imaging [1- 3]. One of the biggest issues regarding the use of organic molecules in biological imaging is the strong absorption in the visible range where light penetration into the tissues is reduced. In this way, Near InfraRed (NIR) dyes have been the subject of numerous studies concerning their application as fluorescent markers. The advantages of using NIR dyes include minimal interfering absorption and fluorescence from biological samples, minimum photo-damaging of the sample under study and enhanced tissue penetration depth [4,5] due to a high molar absorption coefficient (ϵ) in the long wavelength region (600 – 900 nm) where tissue light scattering is lower [6, 7].

Among the variety of organic fluorophores, polymethine dyes and related molecular systems are one of the most commonly used class of molecules for NIR-fluorescent sensor design [6].

NIR-fluorescent dyes based on the rhodamine core (or rhodamines) have been used as laser dyes and fluorescence standards for a long time [8] and also as fluorescence markers in many applications [7, 8], due to their high fluorescence quantum yields, high extinction coefficients, good photostability and usually low quantum yield of triplet state formation. It is also well known that rhodamine dyes can present a fluorescence on-off switching mechanism (when the *o*-carboxylic acid group of rhodamine dyes undergo intramolecular cyclization turning the open form into a spirocyclic one [8], which is non-fluorescent due to the interruption of the π -electron system in the dye's chromophoric structure).

Regarding the mentioned above, we decided to explore the synthesis of new compounds absorbing in the NIR region, composed by an heterocyclic system which bears structural fragments of both rhodamines and benzo[b]pyrilium salts in one single molecular skeleton, the 6-(*N,N*-dialkylamino)-1,2,3,4-tetrahydroxanthylum system.

Although the first examples of these molecules were reported in 1979 (as side products) [9] the dyes derivatives of this heterocyclic framework were synthesized only in 2012 [10]. These compounds (namely unsymmetrical trimethinecyanines from 1,3,3-trimethyl-3H-indolenine and 1,3,3-trimethyl-3H-benzo[e]indolenine) showed excellent photophysical properties, including absorption in the NIR region (688 – 728 nm), large absorption extinction coefficients ($130 - 140 \times 10^3 \text{ M}^{-1}\text{cm}^{-1}$), high fluorescence quantum yields (0.29 – 0.56), good photostability and sufficient chemical stability. It was also reported that these dyes are superior to traditional rhodamine dyes with both absorption and emission in the NIR region, while retaining a very important structural feature such as the rhodamine-like fluorescence ON-OFF switching mechanism [10].

One of the most remarkable features affecting both chemical and photostability of polymethine dyes is their conjugated chain length and type of structure (opened, bridged, etc.). The stability of cyanines increases with the decrease of the number of “opened” methine units (unsaturated carbons) in the conjugated chain. In this way, we decided to focus our attention in the dyes derivatives of the 6-(*N,N*-diethylamino)-1,2,3,4-tetrahydroxanthylum system, bearing only one “opened” conjugated methine atom.

Herein, we describe the synthetic route to eight different dyes and the evaluation of their photochemical parameters namely the absorption and emission wavelength, the fluorescence quantum yields and lifetimes and also the singlet oxygen formation quantum yields. The nature of the electronic transitions was studied by analysing the molecular geometry of the synthesized compounds.

2. Materials and methods

2.1. General

Reagents and solvents used in the synthesis of the dyes were of commercial origin and, unless otherwise stated, used as received. Solvents used in the measurement of spectral-luminescent properties were of spectroscopic grade. 9-(2-Carboxyphenyl)-6-(*N,N*-diethylamino)-1,2,3,4-

tetrahydroxanthylum perchlorate (**1**) [11], 7-(*N,N*-diethylamino)coumarine-3-carbaldehyde (**2h**) [12], 9-(2-carboxyphenyl)-6-(*N,N*-diethylamino)-4-[(3-methylimidazo[1,5-*a*]pyridin-1-yl)methylidanyl]-1,2,3,4-tetrahydroxanthylum perchlorate (**3e**) [13] and 3-phenylimidazo[1,5-*a*]pyridine (**4**) [14] were prepared as previously reported. All reactions were monitored by thin-layer chromatography on aluminium plates pre-coated with Merck silica gel 60 F₂₅₄ (0.25 mm). ¹H and ¹³C NMR spectra were recorded on a Bruker ARX400 spectrometer at room temperature, unless otherwise stated; δ in ppm relative to SiMe₄ or to residual solvent signals, *J* in Hz. IR spectra were obtained on a Unicam Research Series FT-IR spectrophotometer; ν_{\max} in cm⁻¹. High and low resolution Electrospray Ionization Time-of-Flight (ESI-TOF) mass spectra were measured with a VG AutoSpec M spectrometer. Melting points were determined in open capillary tubes in a Buchi 535 melting point apparatus and are uncorrected.

2.2. Synthesis of compounds

2.2.1. 3-Phenylimidazo[1,5-*a*]pyridine-1-carbaldehyde (**2f**)

To a solution of 3-phenylimidazo[1,5-*a*]pyridine (**4**) (1.50 g, 7.73 mmol) in anhydrous *N,N*-dimethylformamide (10 mL), under vigorous stirring at 0-5°C, was added dropwise phosphorus oxychloride (0.72 mL, 7.73 mmol) during 20 min. Once the addition was complete, the reaction mixture was kept at room temperature for 3 h and then poured into 20% aqueous sodium hydroxide (50 mL). The resulting solid was filtered off under reduced pressure, washed with water (40 mL) and recrystallized from propan-2-ol to afford **2f** as greenish-yellow flakes. Yield 82%. Mp 229-231 °C. IR (KBr) ν_{\max} : 700, 768, 968, 1011, 1149, 1286, 1330, 1418, 1500, 1536, 1654, 1879, 2846, 3071. ¹H NMR (400.13 MHz, DMSO-*d*₆): 6.80 (1H, t, *J* = 6.8, ArH), 7.15 (1H, t, *J* = 7.8, ArH), 7.39-7.47 (3H, m, ArH), 7.68 (2H, d, *J* = 7.2, ArH), 8.20 (1H, d, *J* = 9.0, ArH), 8.27 (1H, d, *J* = 7.0, ArH), 10.06 (1H, s, CHO). ¹³C NMR (100.62 MHz, DMSO-*d*₆): 115.5, 119.5, 122.5, 126.3, 128.2, 128.5, 129.0, 129.6, 130.3, 134.3, 139.8, 185.6. MS (ESI-TOF): 223 [M+H]⁺.

2.2.2. *9-(2-Carboxyphenyl)-6-(N,N-diethylamino)-4-[4-(N,N-dimethylamino)benzylidenyl]-1,2,3,4-tetrahydroxanthylum perchlorate (3a). Typical procedure.*

A solution of 9-(2-carboxyphenyl)-6-(N,N-diethylamino)-1,2,3,4-tetrahydroxanthylum perchlorate (**1**) (0.20 g, 0.42 mmol) and 4-(N,N-dimethylamino)benzaldehyde (**2a**) (0.63 g, 0.42 mmol) in freshly distilled acetic anhydride (5 mL) was heated under reflux for 5 min. After cooling to room temperature, the precipitated solid was filtered off under reduced pressure, washed with ethyl acetate and diethyl ether and recrystallized from glacial acetic acid/acetonitrile (5/1, v/v), to afford chromatographically pure shining green crystals. Yield 66%. Mp 267-269 °C (dec.). IR (KBr) ν_{\max} : 619, 710, 823, 924, 1141, 1263, 1315, 1354, 1432, 1519, 1568, 1628, 1720. ^1H NMR (400.13 MHz, DMSO- d_6) δ : 1.21 (6H, t, $J = 6.9$, NCH_2CH_3), 1.65-1.89 (2H, m, CH_2), 2.19-2.29 (2H, m, CH_2), 2.92-2.94 (2H, m, CH_2), 3.09 (6H, s, NCH_3), 3.63 (4H, q, $J = 6.9$, NCH_2CH_3), 6.86-6.91 (2H, m, ArH), 7.18 (1H, d, $J = 9.0$, ArH), 7.29 (1H, br s, ArH), 7.38 (1H, d, $J = 7.6$, ArH), 7.67 (d, $J = 9.0$, 2H), 7.75 (1H, t, $J = 7.5$, ArH), 7.86 (1H, t, $J = 8.0$, ArH), 8.19-8.21 (2H, m, $\text{ArH} + =\text{CH}$), 13.18 (1H, br s, COOH). ^{13}C NMR (100.62 MHz, DMSO- d_6) δ : 12.4, 20.8, 25.4, 26.9, 45.0, 95.5, 111.9, 115.5, 116.5, 121.3, 122.1, 123.0, 128.9, 129.7, 130.0, 130.8, 132.9, 134.2, 134.4, 139.8, 151.7, 154.1, 157.3, 160.1, 163.1, 166.4. HRMS (ESI-TOF) m/z : 507.26409 (M^+ ; $\text{C}_{33}\text{H}_{35}\text{N}_2\text{O}_3$ requires 507.26422).

Dyes **3b-d** and **3f-h** were prepared using a similar procedure. Precipitation of compounds **3f** and **3h** from the reaction mixture required cooling to 0-5 °C overnight. Compounds **3f** and **3g** did not required any additional purification.

2.2.3. *9-(2-Carboxyphenyl)-6-(N,N-diethylamino)-4-[5-(N,N-dimethylamino)tiophene-2-yl)-methylidenyl]-1,2,3,4-tetrahydroxanthylum perchlorate (3b)*

Shining green crystals. Yield 57%. Mp 294-296 °C (dec.). IR (KBr) ν_{\max} : 688, 818, 910, 1070, 1133, 1171, 1251, 1371, 1400, 1446, 1623, 1724. ^1H NMR (400.13 MHz, DMSO- d_6) δ : 1.17 (6H,

d, $J = 6.9$, NCH_2CH_3), 1.65-1.81 (2H, m, CH_2), 2.11-2.35 (2H, m, CH_2), 2.72 (2H, br s, CH_2), 3.35 (6H, s, NCH_3), 3.50 (4H, q, $J = 6.9$, NCH_2CH_3), 6.61 (1H, d, $J = 9.2$, ArH), 6.78-6.81 (2H, m, $\text{ArH} + =\text{CH}_{\text{tiophene}}$), 6.92 (1H, d, $J = 2.0$, ArH), 7.30 (1H, d, $J = 7.5$, ArH), 7.68 (1H, t, $J = 7.5$, ArH), 7.77 (1H, t, $J = 7.5$, ArH), 7.95 (1H, d, $J = 5.0$, $=\text{CH}_{\text{tiophene}}$), 8.13 (1H, d, $J = 7.6$, ArH), 8.46 (1H, s, $=\text{CH}$), 12.82 (1H, br s, COOH). ^{13}C NMR (100.62 MHz, $\text{DMSO}-d_6$) δ : 12.4, 20.0, 21.0, 25.7, 25.8, 42.8, 44.3, 95.8, 111.0, 112.2, 112.5, 112.7, 120.1, 125.9, 127.6, 129.3, 130.2, 130.6, 132.7, 135.0, 136.0, 147.0, 151.0, 151.5, 155.3, 162.1, 166.6, 171.9, 173.5. HRMS (ESI-TOF) m/z : 513.22057 (M^+ ; $\text{C}_{31}\text{H}_{33}\text{N}_2\text{O}_3\text{S}$ requires 513.22064).

2.2.4. *9-(2-Carboxyphenyl)-6-(N,N-diethylamino)-4-[(5-(N-pyrrolidinyl)tiophene-2-yl)-methylidenyl]-1,2,3,4-tetrahydroxanthylum perchlorate (3c)*

Shining green crystals. Yield 52%. Mp 294-296 °C (dec.). IR (KBr) ν_{max} : 710, 771, 845, 907, 1063, 1111, 1154, 1220, 1254, 1310, 1372, 1515, 1546, 1624, 1724. ^1H NMR (400.13 MHz, $\text{DMSO}-d_6$) δ : 1.17 (6H, t, $J = 6.8$, NCH_2CH_3), 1.72-1.80 (2H, m, CH_2), 2.07-2.28 (6H, m, CH_2), 2.73 (2H, br s, CH_2), 3.49 (4H, q, $J = 6.8$, NCH_2CH_3), 3.62 (4H, br s, CH_2), 6.59 (1H, d, $J = 9.2$, ArH), 6.72 (1H, d, $J = 4.9$, $=\text{CH}_{\text{tiophene}}$), 6.77 (1H, dd, $J = 2.2, 9.2$, ArH), 6.90 (1H, d, $J = 2.2$, ArH), 7.31 (1H, d, $J = 7.6$, ArH), 7.68 (1H, t, $J = 7.6$, ArH), 7.79 (1H, t, $J = 7.5$, ArH), 7.97 (1H, d, $J = 4.9$, $=\text{CH}_{\text{tiophene}}$), 8.12 (1H, d, $J = 7.8$, ArH), 8.48 (1H, s, $=\text{CH}$), 12.96 (1H, br s, COOH). ^{13}C NMR (100.62 MHz, $\text{DMSO}-d_6$) δ : 12.4, 20.3, 21.0, 25.2, 25.7, 25.8, 44.3, 52.0, 95.8, 111.8, 112.1, 112.6, 120.1, 126.0, 127.5, 129.3, 129.4, 130.3, 130.6, 132.7, 135.1, 136.1, 147.1, 150.3, 151.3, 155.1, 161.8, 166.6, 169.7, 171.9. HRMS (ESI-TOF) m/z : 539.23623 (M^+ ; $\text{C}_{33}\text{H}_{35}\text{N}_2\text{O}_3\text{S}$ requires 539.23629).

2.2.5. *9-(2-Carboxyphenyl)-6-(N,N-diethylamino)-4-[3-(4-N,N-dimethylaminophenyl)allylidenyl]-1,2,3,4-tetrahydroxanthylum perchlorate (3d)*

Shining green crystals. Yield 79%. Mp 263-265 °C (dec.). IR (KBr) ν_{max} : 704, 1110, 1283, 1364, 1435, 1532, 1628, 1725. ^1H NMR (400.13 MHz, $\text{DMSO}-d_6$) δ : 1.23 (t, $J = 6.8$, NCH_2CH_3), 1.72-

1.80 (2H, m, CH₂), 2.22-2.31 (2H, m, CH₂), 2.67-2.87 (2H, m, CH₂), 3.05 (6H, s, NCH₃), 3.63 (4H, br q, *J* = 6.8, NCH₂CH₃), 6.77 (2H, d, *J* = 8.8, ArH), 6.88 (1H, d, *J* = 9.4, ArH), 7.16-7.20 (2H, m, ArH), 7.29-7.33 (2H, m, ArH), 7.37 (1H, d, *J* = 7.4, ArH), 7.63 (2H, d, *J* = 8.8, ArH), 7.75 (1H, t, *J* = 7.5, ArH), 7.85 (1H, t, *J* = 7.4, ArH), 8.03 (1H, d, *J* = 10.4, ArH), 8.20 (1H, d, *J* = 7.6, ArH), 13.18 (br s, 1H, COOH). ¹³C NMR (100.62 MHz, DMSO-*d*₆) δ: 12.4, 20.4, 21.0, 24.5, 25.8, 45.1, 95.4, 112.1, 115.7, 116.5, 120.0, 121.6, 123.6, 123.9, 129.0, 129.7, 130.0, 130.5, 130.8, 133.0, 134.4, 140.8, 146.6, 151.8, 154.1, 157.2, 160.0, 162.0, 166.4, 171.9. HRMS (ESI-TOF) *m/z*: 533.27953 (M⁺; C₃₅H₃₇N₂O₃ requires 533.27987).

2.2.6. *9-(2-Carboxyphenyl)-6-(N,N-diethylamino)-4-[3-phenylimidazo[1,5-a]pyridin-1-yl)methylidenyl]-1,2,3,4-tetrahydroxanthylum perchlorate (3f)*

Shining green crystals. Yield 47%. Mp 226-228 °C (dec.). IR (KBr) ν_{max}: 697, 824, 997, 1120, 1181, 1259, 1320, 1437, 1533, 1581, 1624, 1811. ¹H NMR (400.13 MHz, DMSO-*d*₆) δ: 1.28 (6H, t, *J* = 6.9, NCH₂CH₃), 1.75-1.84 (2H, m, CH₂), 2.24-2.34 (2H, m, CH₂), 3.38-3.50 (2H, m, CH₂), 3.66 (4H, br q, *J* = 6.9, NCH₂CH₃), 6.88 (1H, d, *J* = 9.4, ArH), 7.14-7.17 (2H, m, ArH), 7.38-4.40 (2H, m, ArH), 7.52 (1H, t, *J* = 7.8, ArH), 7.57-7.66 (3H, m, ArH), 7.75 (1H, t, *J* = 7.6, ArH), 7.83 (1H, t, *J* = 7.5, ArH), 7.94 (2H, d, *J* = 7.4, ArH), 8.20 (1H, d, *J* = 7.8, ArH), 8.49 (1H, s, =CH), 8.54 (1H, d, *J* = 9.0, ArH), 8.70 (1H, d, *J* = 6.9, ArH), 12.96 (1H, br s, COOH). ¹³C NMR (100.62 MHz, DMSO-*d*₆) δ: 12.5, 20.6, 21.0, 25.9, 26.6, 44.9, 95.7, 115.4, 116.1, 116.5, 118.3, 121.5, 121.8, 124.6, 126.3, 128.3, 128.4, 128.8, 129.0, 129.1, 129.7, 129.8, 129.9, 130.8, 132.9, 137.9, 141.7, 153.9, 157.1, 163.2, 166.4, 171.9. HRMS (ESI-TOF) *m/z*: 580.25865 (M⁺; C₃₈H₃₄N₃O₃ requires 580.25947).

2.2.7. *9-(2-Carboxyphenyl)-6-(N,N-diethylamino)-4-[(N-ethylcarbazol-3-yl)methylidenyl]-1,2,3,4-tetrahydroxanthylum perchlorate (3g)*

Shining blue crystals. Yield 67%. Mp 228-230 °C. IR (KBr) ν_{\max} : 624, 758, 937, 985, 1102, 1163, 1233, 1259, 1342, 1377, 1441, 1529, 1572, 1629, 1725, 1812. ^1H NMR (400.13 MHz, DMSO- d_6 , 50 °C) δ : 1.28 (6H, t, $J = 6.8$, NCH_2CH_3), 1.38 (3H, t, $J = 6.8$, NCH_2CH_3), 1.79-1.86 (2H, m), 2.35-2.39 (2H, m, CH_2), 3.10 (2H, br s,), 3.70 (4H, br q, $J = 6.8$, NCH_2CH_3), 4.51 (2H, br q, $J = 6.8$, NCH_2CH_3), 7.01 (1H, d, $J = 9.5$, ArH), 7.25-7.31 (2H, m, ArH), 7.36-7.41 (2H, m, ArH), 7.53 (1H, t, $J = 7.7$, ArH), 7.67 (1H, d, $J = 8.1$, ArH), 7.74-7.80 (2H, m, ArH), 7.86-7.90 (52H, m, ArH), 8.22-8.28 (2H, m, ArH), 8.46 (1H, s, =CH), 8.56 (1H, s, ArH). ^{13}C NMR (DMSO- d_6) δ : 12.5, 13.7, 21.0, 25.4, 26.7, 37.2, 45.3, 95.5, 109.6, 109.7, 116.5, 117.7, 119.7, 120.7, 121.8, 122.2, 122.7, 124.1, 125.3, 126.3, 126.5, 128.9, 129.3, 129.4, 129.6, 130.1, 130.9, 133.0, 134.2, 138.8, 140.1, 140.3, 154.9, 157.8, 161.9, 166.4, 171.9. HRMS (ESI-TOF) m/z : 581.27858 (M^+ ; $\text{C}_{39}\text{H}_{37}\text{N}_2\text{O}_3$ requires 581.27987).

2.2.8. *9-(2-Carboxyphenyl)-6-(N,N-diethylamino)-4-[7-(N,N-diethylamino)benzo[e]pyran-2-on-3-yl)methylidenyl]-1,2,3,4-tetrahydroxanthylum perchlorate (3h)*

Shining green crystals. Yield 70%. Mp 262-264 °C (dec.). IR (KBr) ν_{\max} : 624, 706, 750, 811, 959, 1007, 1115, 1254, 1332, 1385, 1451, 1506, 1564, 1616, 1707. ^1H NMR (400.13 MHz, DMSO- d_6) δ : 1.15 (6H, t, $J = 6.8$, NCH_2CH_3), 1.23 (6H, br t, $J = 6.5$, NCH_2CH_3), 1.74-1.79 (2H, m, CH_2), 2.29-2.32 (2H, m, CH_2), 2.91 (2H, br s, CH_2), 3.49 (4H, br q, $J = 6.8$, NCH_2CH_3), 3.68 (4H, br q, $J = 6.5$, NCH_2CH_3), 6.61 (1H, s, ArH), 6.79 (1H, d, $J = 8.9$, ArH), 6.96 (1H, d, $J = 9.3$, ArH), 7.25-7.28 (2H, m, ArH), 7.40 (1H, d, $J = 7.5$, ArH), 7.59 (1H, d, $J = 8.9$, ArH), 7.77 (1H, t, $J = 7.6$, ArH), 7.88 (1H, t, $J = 7.5$, ArH), 8.01 (s, 1H, ArH), 8.19-8.23 (2H, m, ArH + =CH). ^{13}C NMR (100.62 MHz, DMSO- d_6) δ : 12.3, 20.8, 21.0, 25.4, 26.9, 44.3, 45.4, 95.4, 96.4, 108.4, 109.2, 114.2, 116.7, 118.0, 121.9, 128.1, 128.8, 129.5, 130.2, 130.8, 131.1, 133.1, 144.1, 151.8, 155.1, 156.2, 157.7, 160.2, 160.9, 166.4, 171.9. HRMS (ESI-TOF) m/z : 603.28346 (M^+ ; $\text{C}_{38}\text{H}_{39}\text{N}_2\text{O}_5$ requires 603.28535).

2.3. UV-Visible absorption spectroscopy

Steady-state absorption spectra were recorded with a Camspec M501 double beam scanning UV/Visible spectrophotometer, at room temperature, in the spectral range from 190 to 1100 nm. The optical densities (O.D.) were measured using a UV quartz cuvette (1 cm path length). All the solutions were used at O.D. = 0.6 in dichloromethane.

2.4. Laser-induced luminescence (LIL): fluorescence emission quantum yields determination

Schematic diagrams of the LIL system are presented in reference [15]. A N₂ laser (PTI model 2000, *ca.* 600 ps FWHM, ~1.0 mJ per pulse, 5Hz), was used in the laser-induced luminescence experiments, the excitation wavelength being 337 nm. With this set-up, luminescence spectra were easily acquired by the use of an InGaAs photodiode array detection system (PDA) from Andor, model i-Dus, working at -60 °C. This detector allows the acquisition of signals that arise in the NIR range (700 nm to 1700 nm), and that are not possible to acquire using a normal UV-visible detector. Corrected spectra were obtained by applying a calibration curve to the desired range. The optical density at the excitation wavelength for both the unknown and standard samples was 0.6 in dichloromethane.

The fluorescence quantum yields of the dyes were calculated relative to the standard from the respective average fluorescence peak areas, and the published quantum yield of the standard, which in this case was HITC (1,1',3,3',3',3'-hexamethylindotricarbocyanine) iodide ($\Phi_F = 0.28$ in ethanol).

2.5. Fluorescence lifetimes determination

Fluorescence lifetimes were determined using EasyLife VTM equipment from OBB (Lifetime range from 90 ps to 3 μ s). This technique uses pulsed light sources from different LEDs (630 nm in this case) and measures fluorescence intensity at different time delays after the excitation pulse. In this case a 695 nm cut-off filter was used. The instrument response function was measured using a

Ludox scattering solution. FelixGX software from OBB was used for fitting and analysis of the decay dynamics.

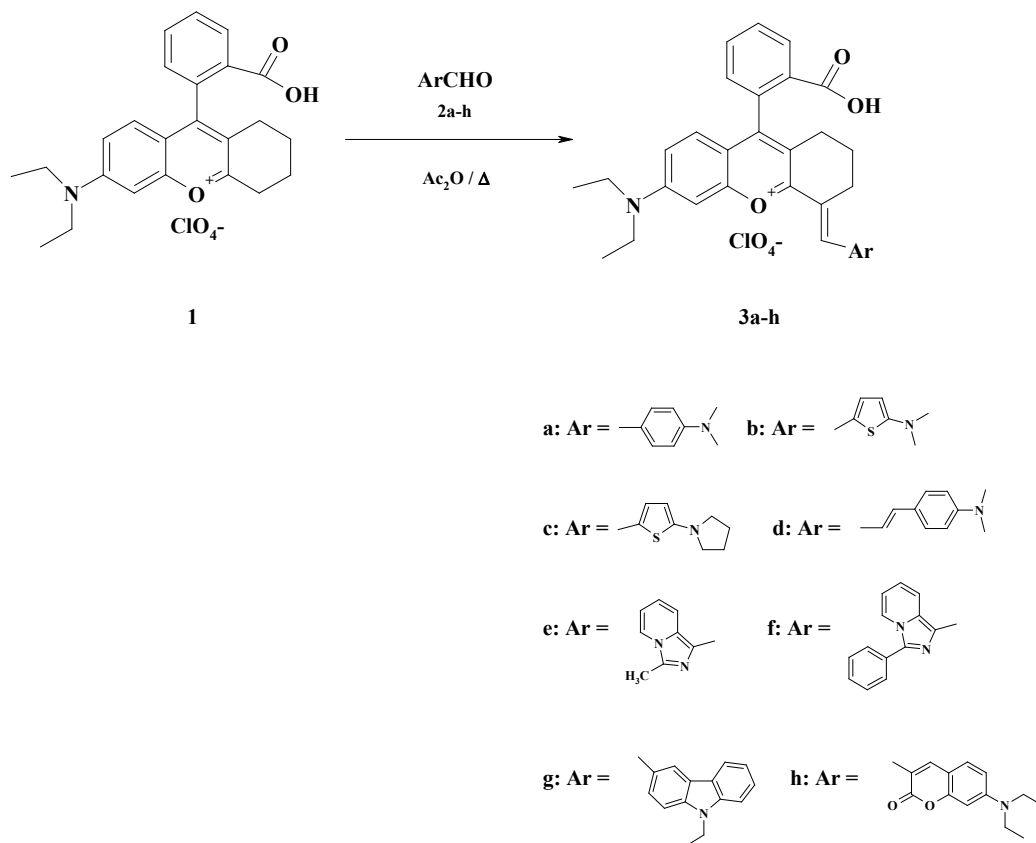
2.6. Singlet oxygen quantum yield determinations

The singlet oxygen measurement set-up was assembled in our laboratory. As an excitation source we used the nitrogen laser described in 2.4. The detector was once again the InGaAs PDA working at low temperature (-60°C) coupled to a fixed spectrograph, model Shamrock 163i also from Andor [16]. The solutions of the dyes were prepared in chloroform with O.D. = 0.6, and phenazine was used as the standard for quantum yields determination.

3. Results and discussion

3.1. Synthesis

The synthesis of the target dyes **3a-h** was carried out by condensation of 9-(2-carboxyphenyl)-6-(*N,N*-diethylamino)-1,2,3,4-tetrahydroxanthylum perchlorate (**1**), prepared by an improved method developed by one of us [11], with several aromatic and heteroaromatic aldehydes (**2a-h**) in refluxing acetic anhydride (Scheme 1). The dyes were obtained in moderate to good yields, crystallizing directly from the crude reaction mixture, in some cases without the need of additional purification.



Scheme 1. Synthesis of dyes **3a-h**.

3.2. Photochemical characterization

All synthesized dyes **3a-h** display strong absorption and emission in the NIR range as depicted in Figure 1.

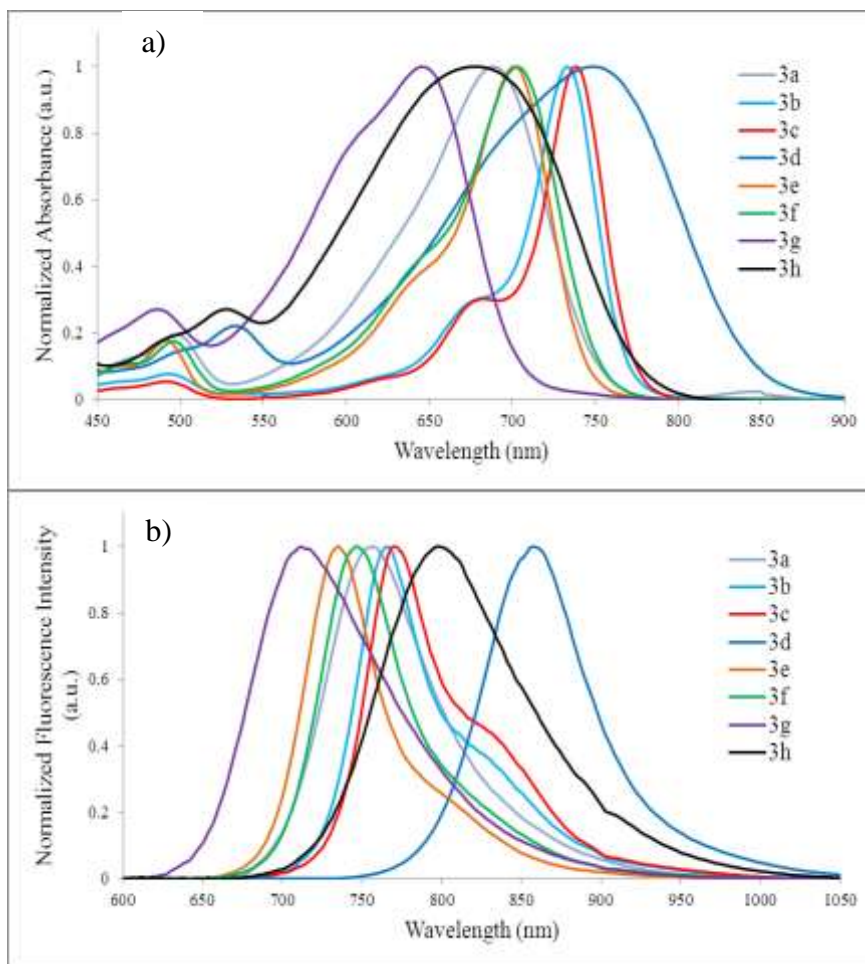


Fig. 1. a) Absorption spectra and b) fluorescence emission spectra of dyes **3a-h** in dichloromethane.

Table 1 summarizes the photochemical parameters obtained for dyes **3a-h**: wavelength of maximum absorption (λ_{abs}) and emission (λ_{em}), molar absorption coefficient (ϵ_{max}), fluorescence emission quantum yield (Φ_{F}), fluorescence lifetime (τ_{F}) and singlet oxygen quantum yield (Φ_{Δ}).

Table 1

Spectral data of dyes **3a-h**.

Dye	$\lambda_{\text{abs}}^{\text{a}}$ (nm)	$\lambda_{\text{em}}^{\text{a}}$ (nm)	Stokes shift (cm^{-1})	$\epsilon_{\text{max}}^{\text{a}}$ ($\text{M}^{-1} \text{cm}^{-1}$)	$\Phi_{\text{F}}^{\text{a}}$	$\tau_{\text{F}}^{\text{a}}$ (ns)	Φ_{Δ}^{b}
3a	689	757	147059	75321	0.04	$0.25 \pm 1.1 \times 10^{-2}$	-
3b	733	766	303030	175894	0.04	$0.17 \pm 8.8 \times 10^{-2}$	-
3c	738	770	312500	156309	0.04	$0.16 \pm 3.5 \times 10^{-4}$	-

3d	749	857	92592	68189	0.20	$1.03 \pm 3.0 \times 10^{-2}$	-
3e	701	735	294117	104000	0.30	$2.21 \pm 4.9 \times 10^{-3}$	0.02
3f	703	746	232558	90000	0.40	$2.97 \pm 2.2 \times 10^{-2}$	0.03
3g	646	712	151515	49000	0.08	$0.79 \pm 1.3 \times 10^{-2}$	0.03
3h	678	797	84034	39000	0.07	$0.36 \pm 7.8 \times 10^{-3}$	0.02

^a In CH₂Cl₂.

^b In CHCl₃.

In a previous work from our group pertaining the study of two “rhodamine-like” hemicyanines derived from the 6-(*N,N*-diethylamino)-1,2,3,4-tetrahydroxanthylum system [17], it was found that the substitution with an aniline fragment in the conjugation chain leads to an increase in the resonance of the molecule which is responsible for the large Stokes shift observed when compared to classical rhodamines. Comparing the dyes under study herein with the “rhodamine-like” dyes described in [17] a considerable deviation of the emission’s wavelength to the red, in some cases more than 100 nm, was observed, which clearly evidences the strong increase in the molecules resonance duo to the influence of the different (hetero)aryl substituents. The most pronounced effect amongst this group of new NIR-absorbing dyes is evident in the spectrum of dye **3d** in which the absorption maximum is located at 749 nm and the emission maximum at 857 nm (Stokes shift of 108 nm).

This type of dyes shows a strong solvatochromic behaviour [13,17]. One of the main consequences of the solute-solvent interactions is, unquestionably, the intramolecular charge transfer (ICT) mechanism, which, in high polarity solvents, can strongly affect the fluorescence quantum yield of the molecule. However, as explored in the aforementioned works of Ferreira et al. and Conceição et al., there should not be a direct correlation between the spectroscopic properties exhibited by these rhodamine-like dyes with the common macroscopic polarity parameters, since both the absorption and emission properties are a consequence of a complex function of polarity, specific solute-solvent interactions, and polarizability of the solvent. Accordingly, dicloromethane,

possessing a Dimroth's ET parameter of 41.1 and a Kosower's Z-value of 64.2, was selected as solvent of choice to minimize these processes due to its relatively low polarity. The fluorescence quantum yields of all compounds under study were calculated relative to HITC iodide as standard. The highest values of Φ_F were obtained for dyes **3d-f**, ranging from 0.20 to 0.40. All dyes exhibited monoexponential fluorescence lifetime decays in dichloromethane in the order of nanoseconds. Dye **3f** presented the highest fluorescence lifetime (~ 3 ns).

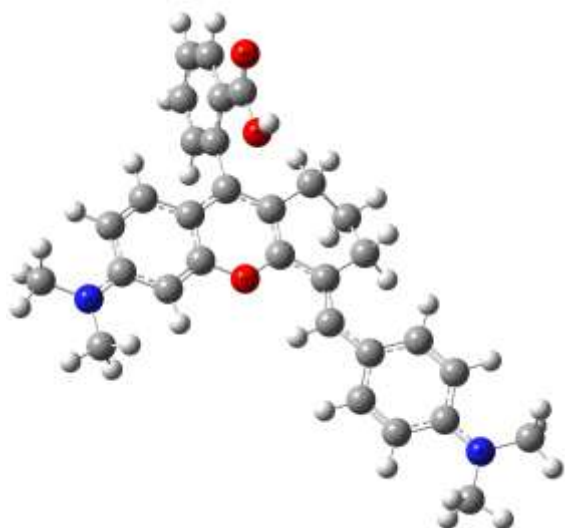
The determination of the singlet oxygen formation quantum yield was performed for all dyes in chloroform by comparison with the singlet oxygen phosphorescence emission of phenazine ($\Phi_\Delta = 0.84$) [18] at 1270 nm. The values obtained are invariably very low and, in some cases, there is no evidence at all of singlet oxygen generation. As reported in literature, rhodamine dyes in general are poor candidates for the formation of excited triplet state because their intersystem crossing ability is very limited [19]. The functionalization of these polymethine dyes seems to have no effect in singlet oxygen production.

The strong absorption and emission in the NIR region and the relatively good fluorescence quantum yields and lifetimes, however, turn dyes **3d-f** good candidates to be used as fluorescence markers in molecular bioimaging techniques.

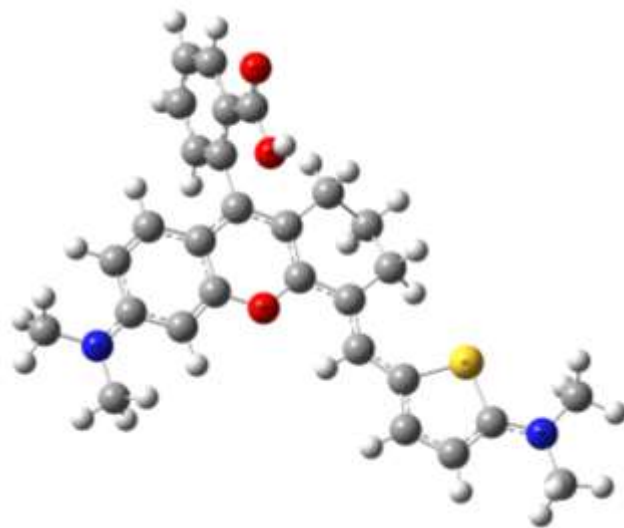
3.3. Spectral properties and the nature of the electronic transitions

In parallel with the spectral study, quantum-chemical calculations for dyes **3a-h** were also carried out. The optimized molecular geometry of the dye molecules in the ground state was obtained by the DFT/6-31G(d,p)/B3LYP method, while the electron-transition characteristics were calculated by the semi-empirical ZINDO/S method using a package Gaussian 03 [20].

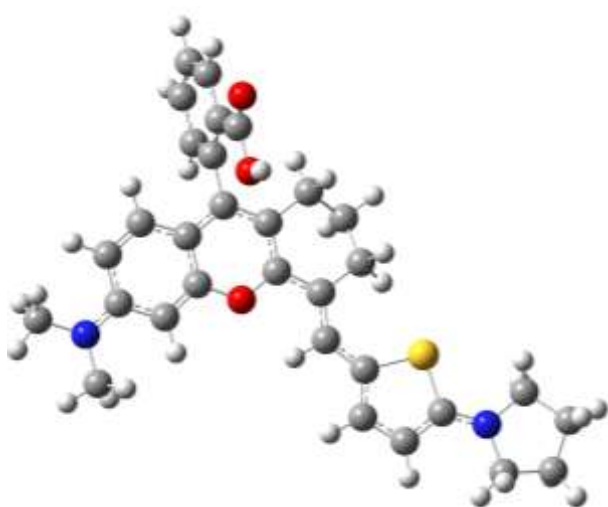
The optimized structures of dyes **3a-h** are shown in Figure 2.



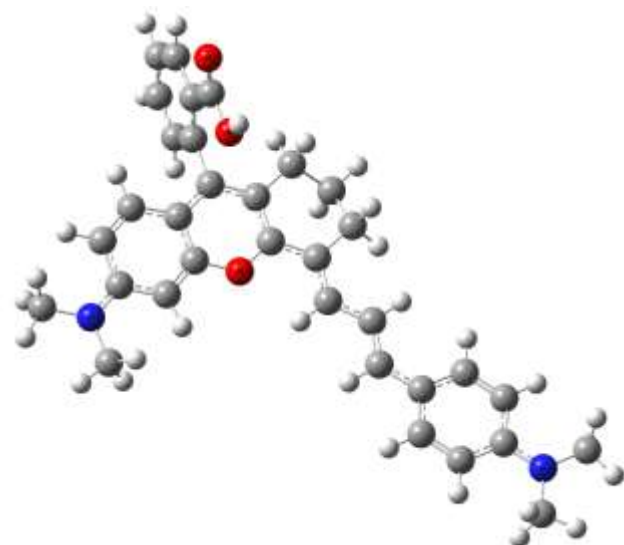
3a



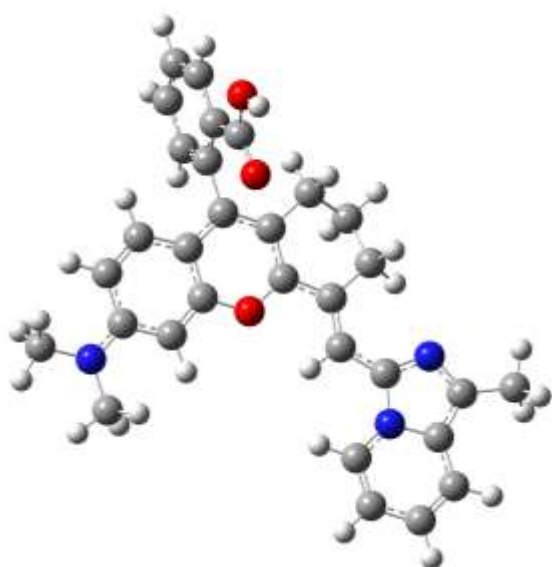
3b



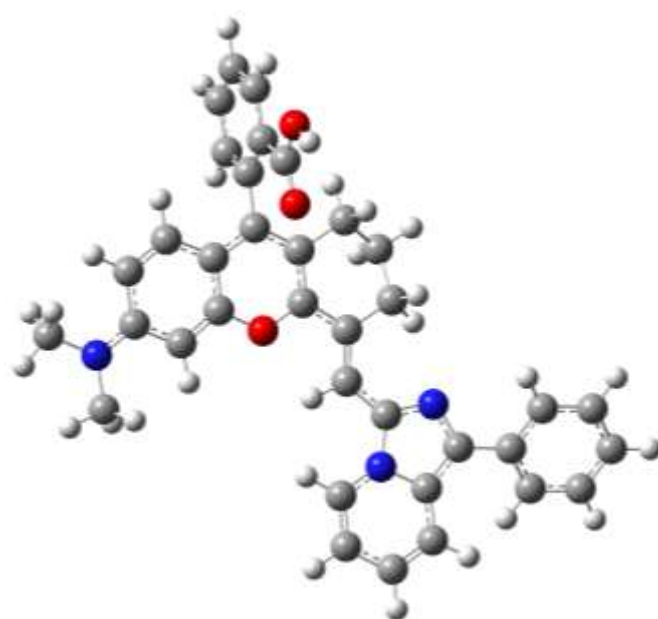
3c



3d



3e



3f

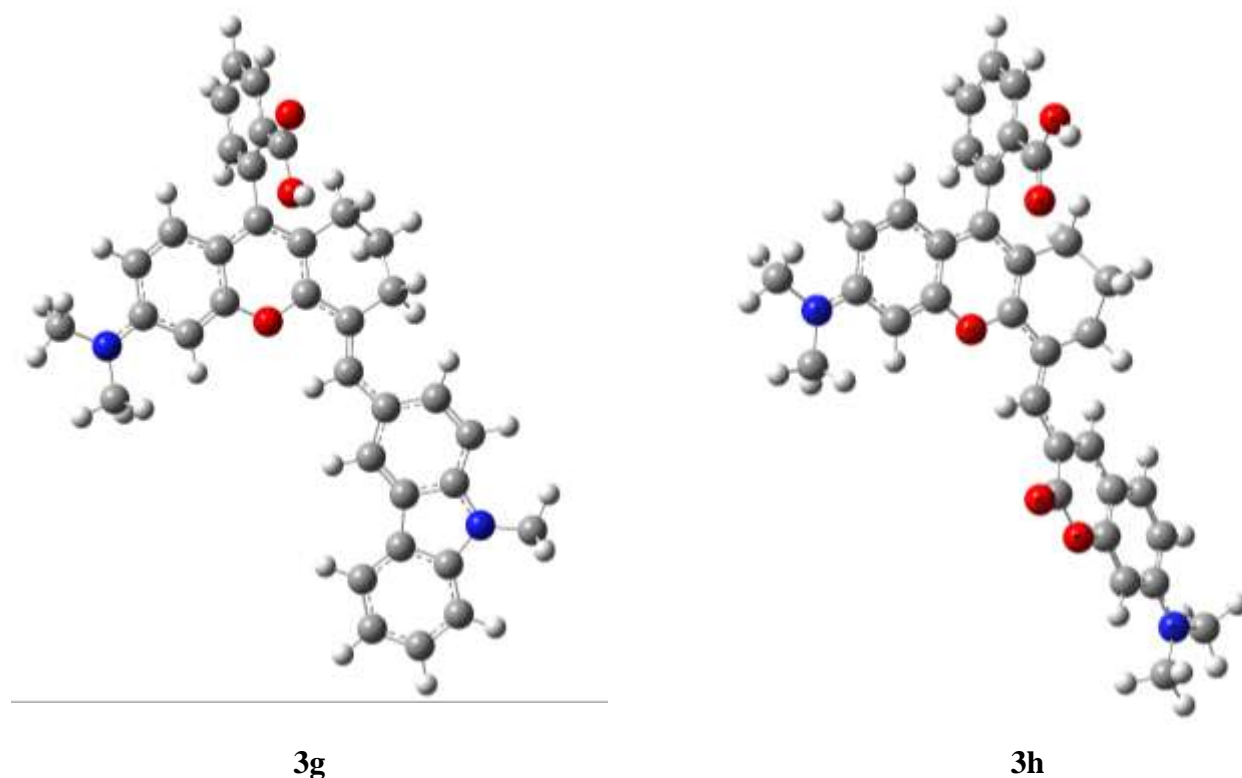


Fig. 2 Molecular geometry of dyes **3a-h**.

In all cases the benzoic acid moiety is highly twisted and essentially positioned vertically in relation to the 1,2,3,4-tetrahydroxanthylum core, with a dihedral angle of nearly 90° ; both π -electron fragments are disposed orthogonally and hence no electronic conjugation exists between them. Contrastingly, following from calculations the aryl substituents and the 1,2,3,4-tetrahydroxanthylum fragment are closely co-planar, excepting the trimethylene bridge. Also, the aryl residues in **3g** and **3h** are somewhat twisted (18°). The phenyl ring in the imidazo[1,5-a]pyridine residue of **3f** is twisted 32° . The replacement of the *N,N*-dimethylamino group in the thiophene substituent of **3b** by the pyrrolidinyl group in **3c** causes only a slight decrease of the valence angle: $\varphi(\text{CH}_3\text{-N-CH}_3) = 120^\circ$ (**3b**) and $\varphi(\text{-CH}_2\text{-N-CH}_2\text{-}) = 112^\circ$ (**3c**).

In spite of these slight distortions of the planar conformation, the strong delocalization of π -electrons is accomplished along the whole quasi-planar conjugated systems, which can be treated as polymethine chromophores, similarly to the well-known cyanine dyes with their equalized carbon-carbon bond lengths. According to the colour theory of polymethine/cyanine dyes, going from dye

3a to its vinyllog **3d** should cause a bathochromic shift of the maximum absorption wavelength of approximately 100 nm (the so-called “vinylene shift”) [21-23]. In this case an experimental bathochromic shift of 60 nm was observed. An alternative way of shifting dyes absorption towards the NIR, avoiding the loss of stability in long open polymethine chains because of twisting around C-C bonds, is the variation of the “effective length” of the terminal groups, for example, replacing the 4-(*N,N*-dimethylamino)phenyl group of dye **3a** by 5-(*N,N*-dimethylamino)thiophenyl in **3b**. The same is observed with the introduction of the 3-methylimidazo[1,5-*a*]pyridine residue (in dye **3e**) or its phenyl-substituted analogue (in dye **3f**). The phenyl group in the aryl substituent of **3f** does not provide experimentally an appreciable spectral effect, although calculations predict a bathochromic shift of 21 nm (Table 2). The carbazole and the coumarine moieties (in dyes **3g** and **3h**, respectively) are not capable of causing a deviation of the dyes absorption towards the NIR, despite both aryl substituents consist of bulky conjugated systems. Inversely, hypsochromic shifts were obtained, reaching -43 nm in the case of dye **3b**; calculations predict a somewhat lower value in this case (-38 nm).

Such modifications of the constitution of the polymethine chromophore result in shifting of electron levels, first of all, the frontier levels involved in the lowest electron transition. The positions of some levels, as well as the shape of the corresponding MOs, are illustrated for dyes **3a,b** and **3d** in Figure 3.

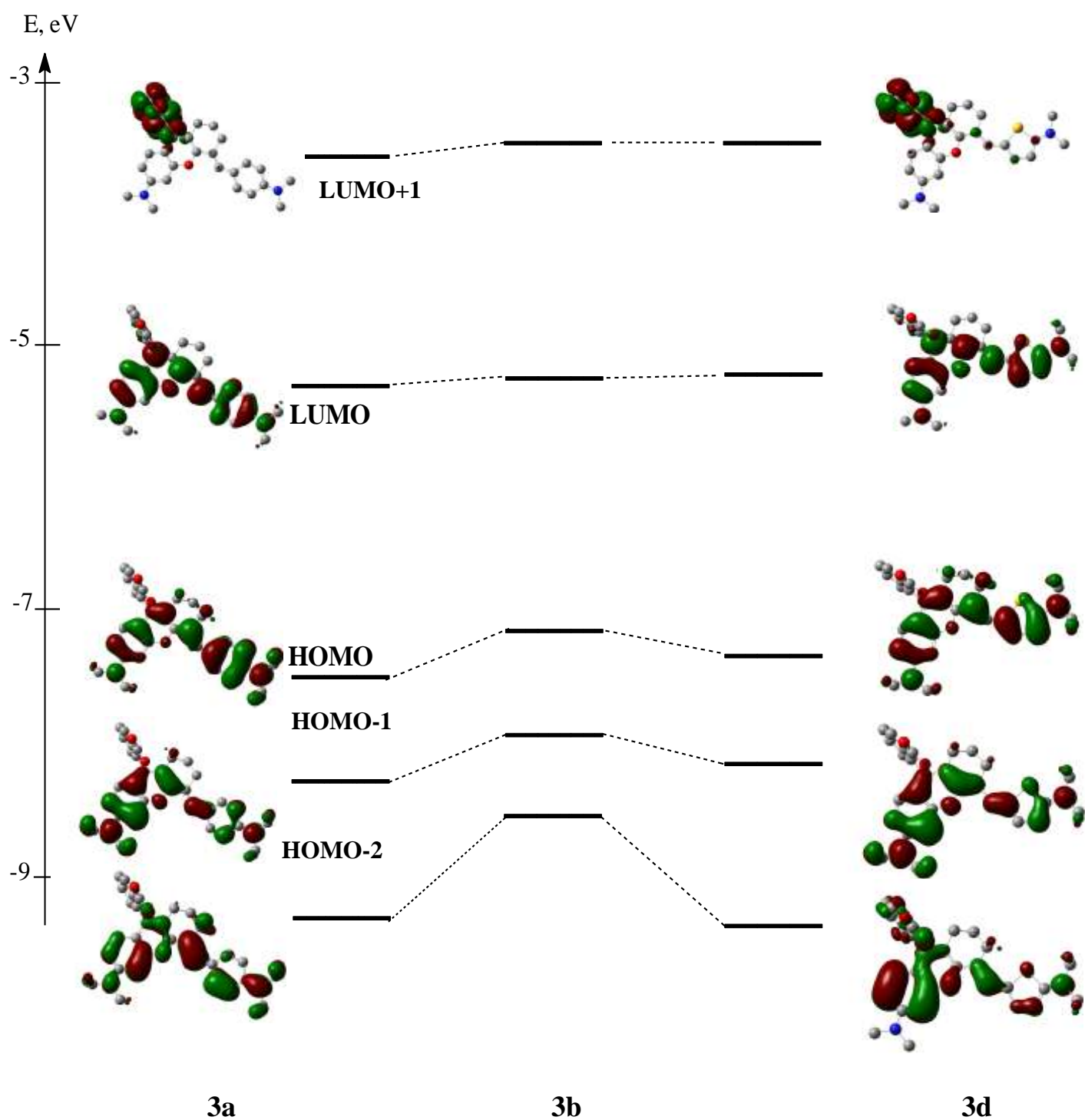


Fig. 3 Positions of electron levels and shape of corresponding MOs for dyes **3a**, **3b** and **3d**.

It is apparent that the lowest vacant orbital and the three highest occupied MOs are uniformly delocalized along the whole chromophore, whereas the next vacant MO (LUMO+1) is

concentrated in the perpendicular substituent. The comparison of the same orbital for the various dyes shows that their shapes remain practically similar.

Contrastingly, the positions of the electron levels are sensitive to the lengthening of the chain and to the structural variation of the terminal groups. Though, the change in the energy of the lowest vacant level is negligible (for example $\epsilon_{\text{LUMO}} = -5,145$ eV in **3a** and $-5,050$ eV in **3b**). The shifting of the occupied levels is shown in Figure 3 to be more appreciable. Also, the energies of the occupied π -MOs located completely within the twisted fragment are lower than the orbitals presented in Figure 3.

To study the nature of the electron transitions in connection with the spectral bands in the visible region, the calculations of the excited states were performed by the semi-empirical ZINDO method (with variation of the Overlap Weight Factor - OWF). It is well known that the TD DFT method gives a significant divergence between the calculated and the experimental wavelengths for the first electronic transitions in polymethine dyes, especially in molecules with extensive linear π -systems [24,25]. It should also be noted that the semi-empirical ZINDO approximation gives more realistic values of the spectral characteristics. A careful comparison of the quantum-chemical results and the experimental data allows obtaining the necessary information for the analysis of the nature of the electron transitions and their intensities. The calculated characteristics for dyes **3a-h** are collected in Table 2.

Table 2

Absorption maxima (λ_{\max}) and oscillator strengths (f) of the lowest electron transitions of dyes **3a-h** calculated by the ZINDO/S method (OWF = 0.45).

Dye	Transition	λ_{\max} (nm)	$\Delta\lambda^b$ (nm)	f
3a	$S_0 \rightarrow S_1$	678 [689] ^a	-	1.098
	$S_0 \rightarrow S_2$	407	-	0.059
	$S_0 \rightarrow S_3$	396	-	0.092
3b	$S_0 \rightarrow S_1$	732 [733] ^a	+ 54 [+ 44] ^a	1.086
	$S_0 \rightarrow S_2$	416	+9	0.130
	$S_0 \rightarrow S_3$	400	+4	0.102
3c	$S_0 \rightarrow S_1$	734 [738] ^a	+ 56 [+ 49] ^a	1.152
	$S_0 \rightarrow S_2$	421	+ 14	0.206
	$S_0 \rightarrow S_3$	404	+ 8	0.075
3d	$S_0 \rightarrow S_1$	776 [749] ^a	+ 98 [+ 60] ^a	1.553
	$S_0 \rightarrow S_2$	444	+37	0.035
	$S_0 \rightarrow S_3$	394	-2	0.327
3e	$S_0 \rightarrow S_1$	712 [701] ^a	+ 34 [+ 12] ^a	1.295
	$S_0 \rightarrow S_2$	391	- 16	0.259
	$S_0 \rightarrow S_3$	372	- 24	0.530
3f	$S_0 \rightarrow S_1$	733 [703] ^a	+ 55 [+ 14] ^a	1.321
	$S_0 \rightarrow S_2$	400	- 7	0.104
	$S_0 \rightarrow S_3$	378	- 18	0.463
3g	$S_0 \rightarrow S_1$	640 [646] ^a	- 38 [- 43] ^a	0.999
	$S_0 \rightarrow S_2$	456	+ 49	0.006
	$S_0 \rightarrow S_3$	400	+ 4	0.218

3h	$S_0 \rightarrow S_1$	680 [678] ^a	+ 2 [- 11] ^a	1.033
	$S_0 \rightarrow S_2$	424	+ 17	0.405
	$S_0 \rightarrow S_3$	390	- 6	0.033

The lowest electron transitions are described for all dyes by the following configurations: $|S_0 \rightarrow S_1\rangle \approx$

$|HOMO \rightarrow LUMO\rangle$; $|S_0 \rightarrow S_2\rangle \approx |HOMO-1 \rightarrow LUMO\rangle$; $|S_0 \rightarrow S_3\rangle \approx |HOMO-2 \rightarrow LUMO\rangle$.

^a Values in square brackets refer to experimental dyes absorption maxima in CH_2Cl_2 .

^b $\Delta\lambda = \lambda_{\max}(\mathbf{3b-h}) - \lambda_{\max}(\mathbf{3a})$.

It can be seen that the first electron transition, $S_0 \rightarrow S_1$, is described in all dye molecules practically by one single excited configuration involving HOMO and LUMO with the larger oscillator strength. Similarly, the one-configurational nature of the first electron transition was shown to be typical for cyanine dyes [23]. The changes in the calculated wavelength of the $S_0 \rightarrow S_1$ transition with the variation of the chemical constitution of the main chromophore agrees (with reasonable accuracy) with the shifts of the long-wavelength band observed in the absorption spectra. Thus, the spectral outcome of replacing the 4-(*N,N*-dimethylamino)phenyl terminal group in **3a** by 5-(*N,N*-dimethylamino)thiophenyl in **3b** is comparable to the effect of lengthening the polymethine chain from dye **3a** to **3d**. Yet, the first way is preferable once the long-wavelength absorption band becomes more sharp and intense, what can be explained by the decrease of vibrational structures in the dyes with shorter open polymethine chains.

Table 2 also shows the spectral effects for the higher electron transitions, but their values are lower, which is in accordance with the experimental results.

4. Conclusions

Several new dyes, derivatives of the “rhodamine-like” 6-(*N,N*-diethylamino)-1,2,3,4-tetrahydroxanthylum heterocyclic system, were prepared by condensation of 9-(2-carboxyphenyl)-6-(*N,N*-diethylamino)-1,2,3,4-tetrahydroxanthylum perchlorate with several aromatic and heteroaromatic aldehydes.

The photochemical characterization of these dyes was obtained regarding the absorption and fluorescence spectra, fluorescence lifetimes and quantum yields and also singlet oxygen formation quantum yield. The new synthesized dyes display strong absorption and emission in the NIR region (between 646 and 749 nm) and reasonably good fluorescence quantum yields and lifetimes in three cases, **3d**, **3e** and **3f**, the latter presenting the highest values ($\Phi_F = 0.40$, $\tau_F = 3$ ns). The singlet oxygen quantum yields are very low which is in accordance with the fact that this family of dyes presents very low values of triplet state quantum yields.

As suggested by quantum-chemical calculations, the (hetero)aromatic substituents introduced in the 1,2,3,4-tetrahydroxanthylum framework are nearly planar and hence conjugated with its chromophoric system. Consequently, the spectral properties of these dyes are strongly dependant on the nature of the substituents.

All the mentioned before turn some of the synthesized dyes good candidates to be used as fluorescence markers for bioimaging techniques.

Acknowledgments

Thanks are due to FCT (Portugal's Foundation for Science and Technology) and FEDER for financial support through the research unit Centro de Química - Vila Real (CQ-VR (UID/QUI/00616/2013)). FCT is also acknowledged for the PhD fellowships for D. P. Ferreira (SFRH/BD/95359/2013) and D. S. Conceição (SFRH/BD/95358/2013).

References

1. Xia T, Li N, Fang X. Single-molecule fluorescence imaging in living cells. *Annu Rev Phys Chem* 2013;64:459–80.
2. Ghoroghchian PP, Therien MJ, Hammer DA, *In vivo* fluorescence imaging: a personal perspective. *Wiley Interdiscip Rev Nanomed Nanobiotechnol* 2009;1:156–67.
3. Zhang X, Bloch S, Akers W, Achilefu S. Near-infrared molecular probes for *in vivo* imaging. *Curr Protoc Cytom* 2012;Unit12.27.

4. Yuan A, Wu J, Tang X, Zhao L, Xu F, Hu Y. Application of near-infrared dyes for tumor imaging, photothermal, and photodynamic therapies. *J Pharm Sci* 2013;102:6-28.
5. Escobedo JO, Rusin O, Lim S, Strongin RM. NIR dyes for bioimaging applications. *Curr Opin Chem Biol* 2010;14:64-70.
6. Johnson I, Spence MTZ, editors. *The molecular probes handbook: a guide to fluorescent probes and labeling technologies*. 11th ed. Life Technologies Corporation; 2010.
7. Luo S, Zhang E, Su Y, Cheng T, Shi C. A review of NIR dyes in cancer targeting and imaging. *Biomaterials* 2011;32:7127-38.
8. Beija M, Afonso CAM, Martinho JMG. Synthesis and applications of Rhodamine derivatives as fluorescent probes. *Chem Soc Rev* 2009;38:2410-33.
9. Feichtmayr F, Oberlinner A. Zum chromogenen Verhalten von 7,8-dihydro-6-h-[1]benzopyrano[3,2-d]xanthenen. *Liebigs Ann* 1979;9:1337-45.
10. Yuan L, Lin W, Yang Y, Chen H. A unique class of near-infrared functional fluorescent dyes with carboxylic-acid-modulated fluorescence on/off switching: rational design, synthesis, optical properties, theoretical calculations, and applications for fluorescence imaging in living animals. *J Am Chem Soc* 2012;134:1200-11.
11. Prostota YA. Convenient method for synthesis of 6-(*N,N*-diethylamino)-9-(2-carboxyphenyl)-1,2,3,4-tetrahydroxanthylum perchlorate. *Chem Heterocycl Compd* 2004;40:116-7.
12. Kirpichënok MA, Baukulev VM, Karandashova LA, Grandberg II. Synthesis and spectral and luminescent properties of 3-formyl-7-dialkylaminocoumarins. *Chem Heterocycl Compd* 1991;27:1193-9.
13. Conceição DS, Ferreira DP, Prostota Y, Santos PF, Vieira Ferreira LF. Photochemical behaviour of a new 1,2,3,4-tetrahydroxanthylum fluorescent dye with “rhodamine-like” structure in liquid media and adsorbed onto a TiO₂ photo-responsive substrate. *Dyes Pigm* 2016;128:279-88.
14. Prostota Y, Kachkovsky OD, Reis LV, Santos PF. New unsymmetrical squaraine dyes derived from imidazo[1,5-a]pyridine. *Dyes Pigm* 2013;96:554-62.

15. Ferreira LFV, Machado ILF. Surface photochemistry: organic molecules within nanocavities of calixarenes. *Curr Drug Discov Technol* 2007;4:229-45.
16. Ferreira DP, Conceição DS, Ferreira VR, Graça VC, Santos PF, Ferreira LFV. Photochemical properties of squarylium cyanine dyes. *Photochem Photobiol Sci* 2013;12:1948-59.
17. Ferreira, D.P., Conceição DS, Prostota Y, Santos PF, Ferreira LFV. Fluorescent “rhodamine-like” hemicyanines derived from the 6-(*N,N*-diethylamino)-1,2,3,4-tetrahydroxanthylum system. *Dyes Pigm* 2015;112:73-80.
18. Redmond RW, Gamlin JN. A compilation of singlet oxygen yields from biologically relevant molecules. *Photochem Photobiol* 1999;70:391-475.
19. Menzel R, Thiel E. Intersystem crossing rate constants of rhodamine dyes: influence of the amino-group substitution. *Chem Phys Lett* 1998;29:237-43.
20. Frisch MJ, Trucks GW, Schlegel HB, Scuseria GE, Robb MA, Cheeseman JR, et al. *Gaussian03; revision B.05*. Pittsburgh PA: Gaussian, Inc.; 2003.
21. Daehne S. Color and constitution: one hundred years of research. *Science* 1978;199:1163-7.
22. Bach G, Daehne S. Cyanine dyes and related compounds. In: Sainsbury M, editor. *RODD's Chemistry of Carbon Compounds*, Amsterdam: Elsevier Science; 1997, vol. IV, p. 383-481.
23. Aleksei DK. The nature of electronic transitions in linear conjugated systems. *Russ Chem Rev* 1997;66:647-64.
24. Fabian J. TDDFT - calculations of Vis/NIR absorbing compounds. *Dyes Pigm* 2010;84:36-53.
25. Jacquemin D, Zhao Y, Valero R, Adamo C, Ciofini I, Truhlar DG. Verdict: time-dependent density functional theory “not guilty” of large errors for cyanines. *J Chem Theory Comput* 2012;8:1255-59.